Journal of Animal Science, 2023, **101**, 1–14
https://doi.org/10.1093/jas/skad215
Advance access publication 23 June 2023
Cell and Molecular Biology

Establishment and characterization of an immortalized bovine intestinal epithelial cell line

Sudan Meng[†,‡], Y.uexin Wang[†], Shuai Wang[†], Weifeng Qian[†], Qi Shao[†], MengyingDou[†], Shujuan Zhao[†], Jianguo Wang[‖], MengyunLi[†], Yongsheng An[†], Lei He,[†] and Cai Zhang[†,$,1,]

[†]Henan International Joint Laboratory of Animal Welfare and Health Breeding, Henan University of Science and Technology, Luoyang 471023, China
[‡]Innovative Research Team of Livestock Intelligent Breeding and Equipment, Longmen Laboratory, Luoyang 471023, China
[‖]College of Veterinary Medicine, Northwest A&F University, Yangling 712100, China
[$]Henan Engineering Research Center of Livestock and Poultry Eerging Disease Detection and Control, Luoyang 471023, China
[1]Corresponding author: zhangcai@haust.edu.cn

Abstract

Primary bovine intestinal epithelial cells (**PBIECs**) are an important model for studying the molecular and pathogenic mechanisms of diseases affecting the bovine intestine. It is difficult to obtain and grow PBIECs stably, and their short lifespan greatly limits their application. Therefore, the purpose of this study was to create a cell line for exploring the mechanisms of pathogen infection in bovine intestinal epithelial cells in vitro. We isolated and cultured PBIECs and established an immortalized BIEC line by transfecting PBIECs with the pCI-neo-hTERT (human telomerase reverse transcriptase) recombinant plasmid. The immortalized cell line (**BIECs-21**) retained structure and function similar to that of the PBIECs. The marker proteins characteristic of epithelial cells, cytokeratin 18, occludin, zonula occludens protein 1 (**ZO-1**), E-cadherin and enterokinase, were all positive in the immortalized cell line, and the cell structure, growth rate, karyotype, serum dependence and contact inhibition were normal. The *hTERT* gene was successfully transferred into BIECs-21 where it remained stable and was highly expressed. The transport of short-chain fatty acids and glucose uptake by the BIECs-21 was consistent with PBIECs, and we showed that they could be infected with the intestinal parasite, *Neospora caninum*. The immortalized BIECs-21, which have exceeded 80 passages, were structurally and functionally similar to the primary BIECs and thus provide a valuable research tool for investigating the mechanism of pathogen infection of the bovine intestinal epithelium in vitro.

Lay Summary

In dairy cattle, the intestine is essential for productivity as it contributes nearly 10% of the total metabolizable energy. The intestinal epithelium is at risk of infection from constant exposure to pathogenic microorganisms, which seriously endangers an animal's health, but no bovine intestinal epithelial cell line has been developed so far for research on intestine -related diseases. Thus, the goal of this study was to create an immortalized cell line from isolated primary bovine intestinal epithelial cells. The expression of an exogenous human telomerase reverse transcriptase (*hTERT*) gene can circumvent the Hayflick limit by maintaining telomere integrity and we used transfection with a plasmid expressing the *hTERT* gene to convert primary intestinal epithelial cells into an immortalized cell line, which we then characterized. The results showed that the immortalized cell line (BIECs-21) was structurally and functionally similar to the primary bovine intestinal epithelial cells (BIECs) and thus provided a valuable research tool for investigating the mechanism of pathogen infection of the bovine intestinal epithelium in vitro.

Key words: bovine intestinal epithelial cell, immortal, *hTERT*, *Neospora caninum*

Abbreviations: BIECs-21, immortalized bovine intestinal epithelial cell line; CCK-8, cell counting kit-8; CK18, cytokeratin 18; DAPI, 4′,6-diamidino-2-phenylindole; DMEM, Dulbecco's modified Eagle's medium; FBS, fetal bovine serum; G418, geneticin; GLUT2, glucose transporter 2; GLUT5, glucose transporter 5; GPR41, G protein-coupled receptor 41; GPR43, G protein-coupled receptor 43; hTERT, human telomerase reverse transcriptase; IECs, intestinal epithelial cells; MCT-1, monocarboxylate transporter-1; MCT-4, monocarboxylate transporter-4; Nc, *Neospora caninum*; PBIECs, primary bovine intestinal epithelial cells; PBS, phosphate buffered saline; qRT-PCR, quantitative reverse transcription polymerase chain reaction; SCFAs, short-chain fatty acids; SGLT1, sodium-glucose cotransporter 1; SLC, solute carrier; SLC5A8, sodium-dependent monocarboxylate transporter; TEM, transmission electron microscopy; ZO-1, zonula occludens protein 1

Introduction

The intestine is an important organ for the body to digest and absorb nutrients, as well as the largest immune organ, mainly involved in mucosal immunity (Oswald, 2006). The intestine is lined with a continuous single-cell layer of intestinal epithelial cells (**IECs**), which separates the intestinal mucosa from the intraluminal environment and is the largest physical barrier in the body (Tang et al., 2016). The intestinal epithelium is constantly exposed to pathogenic bacteria, viruses, parasites, and other pathogens, posing a serious threat to the health of livestock and poultry (Kogut et al., 2020). IECs are an important tool for studying the pathogenesis of diseases related to intestinal infection; however, it is difficult to obtain and grow primary IECs stably, and this has led to the use of intestinal cell lines as substitute models for primary IECs in

Received March 30, 2023 Accepted June 22, 2023.

most in vitro studies of intestinal disease (O'Sullivan et al., 2017). The establishment of small intestinal epithelial cell lines is essential for understanding the molecular mechanism of intestinal pathogenesis. At present, intestinal epithelial cell lines have been successfully established for humans, pigs, mice, and rats (Emami et al., 1989; Whitehead et al., 1993; Quaroni and Beaulieu, 1997; Zakrzewski et al., 2013; Wang et al., 2014).

Immortalization refers to the process of modifying cultured cells in vitro to prevent senescence through spontaneous mutations or external factors such as virus transfection, radiation, the use of protooncogenes or tumor suppressor genes, and telomerase transfection to achieve unlimited proliferation potential (Piñeiro-Ramil et al., 2019). In normal body cells, telomeres gradually shorten with each division and when they become too short to protect the DNA at chromosome ends, cells enter the stage of aging and death (Kaul et al., 2021). However, in some cancer cells, the telomeres are continuously elongated by telomerase and the cells are able to proliferate indefinitely (Tian et al., 2020). Normal cells cultured in vitro also have proliferation limits, which are called "Hayflick limits" (Hayflick, 1997). Only a few of them, under the influence of certain factors, can activate telomerase to synthesize telomere DNA from their own RNA as a template to supplement or extend telomeres and restore chromosome stability, so that cells can escape the aging process and become immortal (Blackburn, 1991).

The current techniques for immortalizing cells include virus transfection, radiation, the use of protooncogenes or tumor suppressor genes, and telomerase transfection (Guo et al., 2022a). Telomerase activation is an important step in various cell immortalization methods (Wu et al., 2017; Li et al., 2018). However, human telomerase reverse transcriptase (**hTERT**), a catalytic subunit of human telomerase, is a key rate-limiting factor of telomerase activity (Shay et al., 1997). The expression of an exogenous *hTERT* gene in epithelial cells significantly enhances its proliferation ability and circumvents the Hayflick limit (Wang et al., 2022a); therefore, using *hTERT* overexpression to obtain immortalized cell lines is a very reliable method. Nutritional metabolism plays an important role in dairy cattle productivity because the intestine contributes nearly 10% of the total metabolizable energy intake of cows (Monteiro et al., 2022). However, the intestinal epithelium is constantly exposed to a wide range of potential pathogenic microorganisms, which seriously endangers the animals' health. IECs are important for studying intestinal infections, but so far, no bovine intestinal epithelial cell line has been developed for research on intestine-related diseases by transfecting duodenal epithelial cells with the *hTERT* gene.

Neospora caninum (**Nc**) is an obligate intracellular parasite that can infect a variety of animals and neosporosis is one of the main causes of abortions and stillbirths in pregnant cattle (Tao et al., 2022). After being ingested through feed or drinking water, the infective oocysts rupture in the digestive tract releasing sporozoites which parasitize the intestine (Cruz-Vázquez et al., 2017). The sporozoites invade IECs and transform into tachyzoites, which can spread to all parts of the body through the blood and infect a variety of nucleated cells.

The goal of this study was to develop a bovine intestinal epithelial cell line as a model for in vitro investigation of intestinal diseases. We isolated primary bovine intestinal epithelial cells (**PBIECs**) and converted them into an immortalized bovine intestinal epithelial cell line by transfection with a plasmid carrying the *hTERT* gene. The present study hypothesized that an immortalized bovine intestinal epithelial cell line would be successfully established by transfection of PBIECs with a plasmid carrying the *hTERT* gene, and that this cell line could serve as a model for in vitro investigation of intestinal diseases.

Materials and Methods

Animal experiments were performed in accordance with the Helsinki Declaration, with approval by the Ethical and Welfare Committee for Animal Experiments of Henan University of Science and Technology (approval code: 2022533).

Isolation and culture of PBIECs

PBIECs were isolated from the intestinal epithelial tissue of a 1-d-old Holstein calf, which was purchased from a dairy farm in Luoyang, China. A 10-cm segment was excised from the duodenum after euthanasia, and rinsed five times with ice-cold phosphate-buffered saline (**PBS**; Solarbio, Beijing, China) containing 100 IU/mL streptomycin-penicillin (Sigma-Aldrich, Saint Louis, MO, USA). The intestinal segment was ligated with cotton thread, cold PBS with streptomycin–penicillin was injected into it, and it was transferred to the biosafety cabinet within 30 min. The segment was cut open longitudinally, spread on a plate, and a small amount of high-glucose Dulbecco's modified Eagle's medium (**DMEM**, Thermo Fisher Science Inc., Waltham, MA, USA) was poured over it to keep the tissue moist. The intestinal mucosa was scraped off using two scalpels, and the tissue was minced into ~1 mm^3 pieces. The intestinal mucosa tissues were digested with type I collagenase (1 mg/mL; Solarbio) at 37 °C for 40 min; the ratio of collagenase to tissue was 3:1 by volume. Dulbecco's modified Eagle's medium containing 10% fetal bovine serum (**FBS**, Thermo Fisher Science Inc.) was added to terminate enzymatic digestion. The cells were collected by passing the suspension through a 100-μm cell sieve, and washed three times with DMEM containing 10% FBS and 100 IU/mL streptomycin–penicillin, and collected by centrifugation (3K15; Sigma Laborzentrifugen GmbH, Harz, Germany) at 4 °C for 5 min at 100 × *g*. The cells were resuspended in DMEM containing 10% FBS, 1 μM bovine insulin, 1 μM dexamethasone, 2 mM glutamine and100 IU/mL streptomycin–penicillin, seeded into 25 cm^2 culture flasks (Corning, New York, USA), and incubated at 37 °C in a 5% CO_2 incubator. For subculturing, the cells were detached with 0.25% trypsin (Servicebio, Wuhan, China) when the cell growth density reached 80% (2 to 3 d), and the cells were purified by the phase-difference adhesion method (Chen, 2019; Wang et al., 2022a). The single-cell suspensions were digested with 0.25% trypsin, seeded in a 6-well plate and cultured. After 30 min, the medium was carefully removed and put into a new 6-well plate. This operation was repeated three times. The purified cells were used in subsequent experiments.

Plasmid transfection, screening and establishment of the immortalized cell line

The purified cells were passaged once, and when the PBIECs reached 90% confluence, they were transfected with 2 μg of pCI-neo-hTERT recombinant plasmid (containing hTERT) for 24 h at 37 °C with 7.5 μL Lipofectamine 3000 and 5 μL of P3000 reagent (Thermo Fisher Scientific, Shanghai, China). The plasmid was donated by Dr. Lei He of Henan University

of Science and Technology. The medium was replaced with fresh complete medium, and 500 μg/mL of geneticin (**G418**; Beyotime Biotechnology, Shanghai, China) was added to select positive cell clones, which were expanded by culturing at 37 °C. After testing negative for mycoplasma, the newly established cell line, BIECs-21 (passage 36) was sent to the China General Microbiological Culture Collection Center for preservation (CCTCC No. 45029). The BIECs have currently exceeded passage 80, which qualifies them as an "immortal" cell line by current standards (Sauriol et al., 2020).

Cell growth curves and effect of short-chain fatty acids on viability

Unless otherwise stated, PBIECs and BIECs-21 used in all subsequent experiments were at passage 3 and passage 36, respectively. The PBIECs and BIECs-21 were seeded in 96-well plates at a density of 1×10^4 cells/mL with 100 μL of cell suspension per well. Six replicates were set up per day for each treatment group, and viable cell counts were done every day with a cell counting kit-8 (**CCK-8**; Solarbio) following manufacturer's instructions. CCK-8 reagent (10 μL) was added to each well, and the absorbance was measured at 450 nm with a microplate reader (Thermo Fisher Science Inc.) after 1 to 4 h of incubation at 37 °C. The cell growth curves were drawn with time on the x-axis and mean A450 on the y-axis.

To determine the effect of short-chain fatty acids (**SCFAs**) on cell viability, the BIECs-21 were seeded in 96-well plates at a density of 1×10^4 cells/mL with 100 μL of cell suspension per well. After culturing 24 h, the cells were incubated with SCFAs at 0, 30, 60, 90, 120, 150, and 180 mM for 24 h with six replicates in each group. SCFAs consisted of a mixture of sodium acetate, sodium propionate, and sodium butyrate (Macklin, Shanghai, China) at a concentration ratio of 14:5:1. Viable cell counts were done by the CCK-8 method. Cell viability was determined based on the following formula: cell viability (%) = $[(A_{sample} - A_{blank})/(A_{control} - A_{blank})] \times 100$, where A is average absorbance at 450 nm and the blanks were culture medium and CCK-8 solution without cells.

To determine the effects of serum concentration on cell viability, the PBIECs and BIECs-21 were seeded in 96-well plates at a density of 1×10^4 cells/mL with 100 μL of cell suspension per well and cultured for 12 h. Cells were incubated in medium containing FBS at different concentrations (0%, 5%, 10%, and 20%) for 48 h with six replicates in each group and cell viability was measured by the CCK-8 method.

Cell characterization by immunofluorescence detection of selected proteins

The PBIECs and BIECs-21 were seeded on sterile cover slips in 24-well plates at a density of 5×10^4 cells/mL with 1 mL of cell suspension per well. The samples on the sterile cover slips were fixed with formaldehyde at –20 °C for 10 min. Subsequent procedures were performed according to the research methods in the literature (Franke et al., 1979; Zhou et al., 2019). Formaldehyde-fixed cells were permeabilized with 0.1% Triton X-100 for 10 min at room temperature, blocked with 10 g/L bovine serum albumin (Solarbio) for 10 min, and incubated with the primary antibody (anti-cytokeratin 18 rabbit pAb, Servicebio; ZO-1 polyclonal antibody 1, Invitrogen, Shanghai, China; occludin polyclonal antibody, Invitrogen; 1:200) overnight at 4 °C. After washing three times with PBS, the secondary antibody (donkey anti-rabbit IgG antibody; 1:500; Abcom, Shanghai, China) was added and incubated at room temperature for 4 h. The cell nuclei were stained with DAPI (Solarbio) for 5 min at room temperature, and cells were observed and digitally imaged with a fluorescence microscope (Olympus, Tokyo, Japan).

Gene expression analysis by quantitative reverse transcription polymerase chain reaction (qRT–PCR)

The PBIECs and BIECs-21 were seeded in 6-well plates at a density of 2×10^5 cells/mL with 2 mL of cell suspension per well. Total RNA was isolated with TRIzol (Beijing Solarbio Technology Co.) following kit instructions (TaKaRa Bio, Dalian, China). RNA concentration and purity were determined by NanoDrop ND-2000 spectrophotometer (Thermo Fisher Scientific, Wilmington, NC, USA) and integrity was assessed by electrophoresis on 1% agarose. Aliquots of total RNA were reverse-transcribed into cDNA using the HiScript III RT SuperMix for qPCR (+gDNAWiper) kit (Vazyme, Nanjing, China). The ChamQ Universal SYBR qPCR master-mix kit was used (Vazyme) for qRT–PCR. The qRT–PCR conditions were as follows: 95 °C for 3 min, followed by 39 cycles of 95 °C for 10 s, 58 °C for 30 s, and 72 °C for 30 s, and lastly a hold at 4 °C. In this experiment, β-actin was used as the internal control. The PCR primer sequences and target gene sizes are shown in Table 1. The Ct value was determined using Excel, and the relative expression level of mRNAs was calculated using the $2^{-\Delta\Delta Ct}$ method (Zhang et al., 2022), where $\triangle\triangle Ct = (Ct_{\text{Experimental group target gene}} - Ct_{\text{Experimental group β-actin}}) - (Ct_{\text{Control group target gene}} - Ct_{\text{Control group β-actin}})$.

Transmission electron microscopy (*TEM*) to evaluate cell morphology

Cells in monolayers were detached with trypsin, collected by centrifugation at 200 g for 15 min, and washed with precooled PBS. Cells were fixed with 2.5% glutaraldehyde (pH 7.4) for 1 h, washed with precooled PBS, and fixed with 10 g/L osmic acid for 2 h. After dehydration with increasing concentrations of ethanol, the samples were embedded in epoxy resin, sectioned, and stained with a uranium salt. Cells were observed under a transmission electron microscope, and images were collected (Hitachi, Tokyo, Japan).

Karyotypic analysis

The number of chromosomes in BIECs-21 was determined by a standard method (Ho et al., 1987; Wang et al., 2019). When BIECs-21 reached 80% confluence, the cells were incubated with 0.1 μg/mL colchicine (Solarbio) at 37°C for 6 h. Cells were trypsinized and collected by centrifugation at 200 g for 5 min. Cells were resuspended in 75 mM KCl at room temperature, held for 8 min, and mixed with Carnoy's solution (methanol:glacial acetic acid, 3:1 v/v) at 4 °C before collection by centrifugation at 200 g. This step was repeated twice, and 100 μL of cell suspension was pipetted onto a precooled slide and air dried. The cells were digested with 2.5 g/L trypsin plus 0.2 g/L EDTA at 30 °C for 10 to 20 min. Chromosomes were stained with Giemsa dye (Solarbio) for 10 min, then samples were dehydrated, cover slipped, and sealed. The number of chromosomes in metaphase (n = 100 cells) was determined microscopically and digitally imaged.

Measurement of glucose uptake

The PBIECs and BIECs-21 were seeded in 6-well plates at 2×10^5 cells/mL with 2 mL of cell suspension per well. The cells were divided into three groups with six replicates per

Table 1. Primer sequences and amplicon sizes for quantitative real-time PCR

Gene	Accession number	Primer sequence (5′→3′)	Length (bp)
hTERT	NM-001193376.3	F: 5′ AAACCTTCCTCAGCTATGCCC 3′ R: 5′ GCACACATGCGTGAAACCTG 3′	219
*CK*18	NM-001192095.1	F: 5′ GGAAGTGGAGGCCCGATATG 3′ R: 5′ GCGTCGCCAAGACTGAAATC 3′	210
E-cadherin	NM-001002763.1	F: 5′ ATCCAGAAACGGGTGCCATT 3′ R: 5′ GTGGCAGGTGGAGAACCATT 3′	121
Enterokinase	XM-027545460.1	F: 5′ TGGAAACTCATCCGTGCCAA 3′ R: 5′ CGTCTGCAGTAGAACCCGTA 3′	333
Vimentin	NM-173969.3	F: 5′ GCGCTCAAAGGGACTAACGA 3′ R: 5′ GCACAAGGCGTCTTCGGTAA 3′	625
Villin	NM-001191121.2	F: 5′ GAGGAGTGAACACCACACCAG 3′ R: 5′ GCACCATCTGCAGGTTCTCAATG 3′	448
MCT-1	NM-001037319.1	F: 5′ GCTACGTGACTAGCCGGG 3′ R: 5′ GCAGTTCAAATCCAAGTATCGTTAT 3′	165
MCT-4	NM-001109980.3	F: 5′ GAGCGGCAGCAGGGAG 3′ R: 5′ GTCCTGACAGAGGCTGTTCC 3′	152
*GPR*41	NM-001145233.1	F: 5′ GATGGCAGGAGGAAGTGGC 3′ R: 5′ TAGCAAGAGCACGTCCACAG 3′	182
*GPR*43	NM-001163784.1	F: 5′ CGAAGGAAGACAAGGACAGCC 3′ R: 5′ GATTAGACAGCTCCCAGCGG 3′	256
*SLC5A*8	NM-001164861.1	F: 5′ GAGGAACCTTCACGTGGACC 3′ R: 5′ CCAAGTAAGGCATGAGCTGGT 3′	237
*SGLT*1	NM-174606.2	F: 5′ GAGCTCATGCCCAATGGACT3′ R: 5′ AACAACCGTCCTGCGATCAT 3′	173
*GLUT*2	XM-019959659.1	F: 5′ AGGACTCTACTGTGGGCTGAT 3′ R: 5′ AGGATGTGCCATAGCTCGTG 3′	180
GLUT5	NM-001101042.2	F: 5′ CCATTCATCCAAGTGGGCCT 3′ R: 5′ GTCGACGGTGGAAACTCCTT 3′	203
β-Actin	NM-173979.3	F:5′ CCGCAACCAGTTCGCCAT 3′ R: 5′ AGGGTCAGGATGCCTCTCTT 3′	216

group: cell medium containing low glucose only (control group), PBIECs cultured with low glucose, and BIECs-21 cultured with low glucose. After culturing for 24 h, the culture supernatants were collected and glucose concentration was measured with a glucose test kit (hexokinase) (Nanjing Jiancheng Bioengineering Institute, Jiangsu, China).

Analysis of contact inhibition

The BIECs-21 were seeded in a 6-well plate at 2×10^5 cells/mL with 2 mL of cell suspension per well. The appearance of cells approaching confluence and at confluence was observed under a microscope (Olympus).

Establishment of a *Neospora caninum* infection model in BIECs-21

Confluent BIECs-21 were infected with Nc-1 or GFP-Nc at a MOI of 3:1 (parasite:cell) for 24 h. The Nc-1 and GFP-Nc were donated by Professor Qun Liu of the College of Veterinary Medicine, China Agricultural University. The growth and morphology of Nc-1 and GFP-Nc on BIECs-21 was imaged with an inverted microscope (Olympus).

Statistical analyses

Results are given as mean ± SD. Differences between groups were compared by IBM SPSS v19.0 and visualized with GraphPad Prism8. Statistical significance ($P < 0.05$) was determined by Student's *t* test for the assays of SCFA and glucose uptake, and calculated by one-way analysis of variance (ANOVA) with a Duncan test on the effect of SCFAs on viability and the serum dependence of PBIECs and BIECs-21.

Results

Isolation and culture of primary BIECs and subculture of BIECs-21

We isolated PBIECs from bovine intestinal epithelial tissue using 0.2% type I collagenase. The cell viability was 97% as estimated by trypan blue staining (Solarbio). Some cells adhered in the form of cell clusters within 48 h post-isolation, and cells constantly migrated around the cell masses. A large number of single cells did not adhere on the bottom of culture plate (Figure 1A). After 72 h, a number of cells migrated out of the cell mass, divided and spread around, showing clonal growth and high refractive index (Figure 1B). After 5 to 7 d, the cells fused into islands, and assumed a flat polygonal shape. Epithelial cells were mixed with fibroblasts (Figure 1C).

After purification by the method of phase-difference adhesion, the adherent cells were uniform in size, flattened and polygonal, arranged in a tight monolayer (Figure 1D). The purified cells were used in subsequent experiments. There

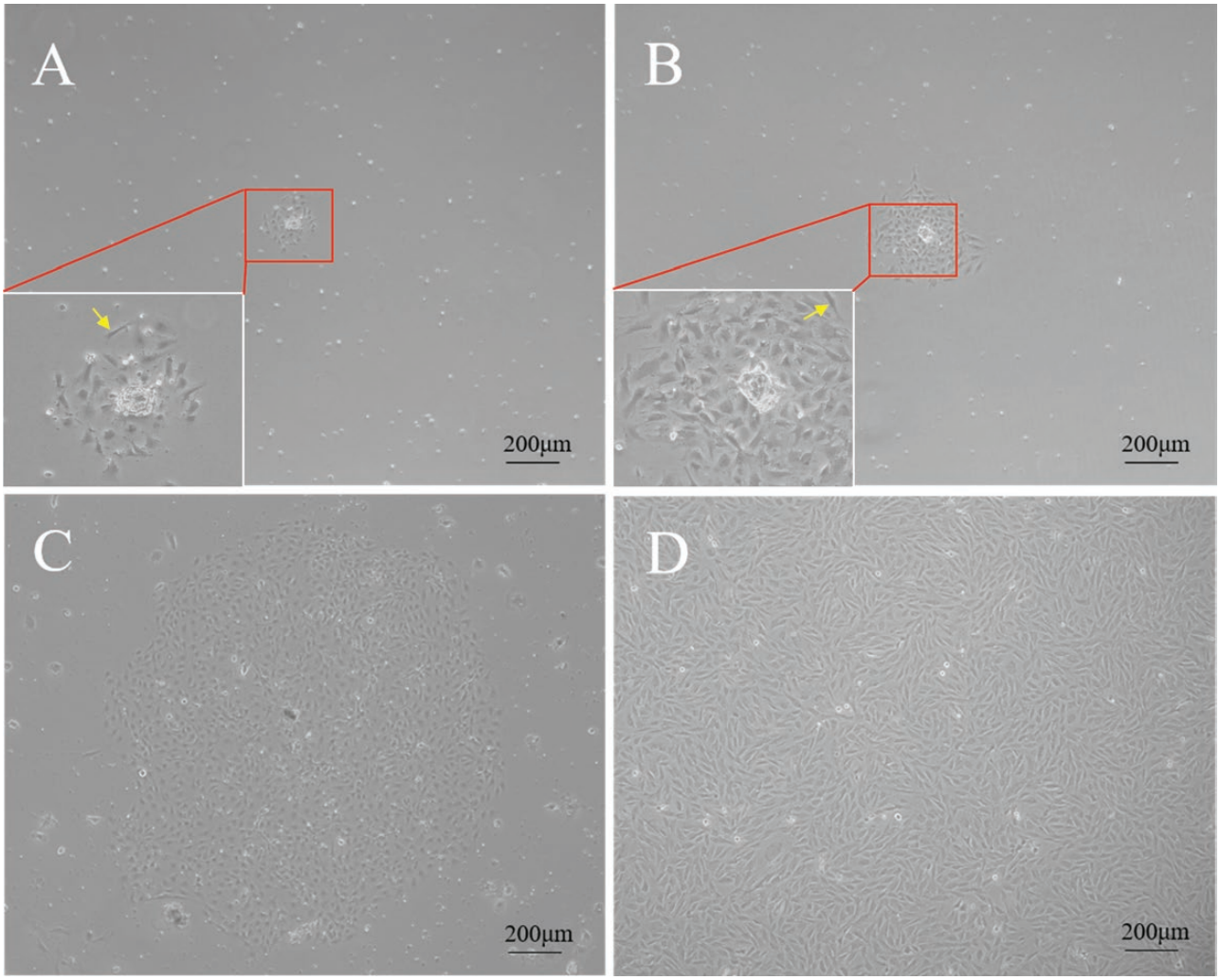

Figure 1. Primary and purified cultures of PBIECs. (A, B, and C) PBIECs cultured for 48 h, 72 h, and 5 to 7 d (50×), fibroblasts are indicated by arrows; (D) purified PBIECs (50×). PBIECs: primary bovine intestinal epithelial cells.

was no significant difference in morphology of immortalized BIECs with G418 at passages 5, 9, 14, 21, 28, and 36 after *hTERT* transfection (Figure 2).

Identification of PBIECs and BIECs-21

The PBIECs and BIECs-21 were immunostained for the epithelial markers, cytokeratin 18 (**CK18**), occludin and zonula occludens-1 (**ZO-1**) as described in Methods. Red fluorescence indicates the CK18 and occludin proteins and green fluorescence shows the ZO-1 protein. The marker proteins characteristic of epithelial cells, CK18, occludin and ZO-1, were all positive in both primary (Figure 3A to C) and immortalized cells (Figure 3D to F). No significant positive staining was observed in the negative controls without antibody (Figure 3G to I). DAPI was used to stain the nuclei blue. The expression of mRNA for the intestinal epithelial marker proteins enterokinase and villin, and epithelial marker proteins *CK*18, E-cadherin, and the fibroblast marker proteins vimentin, and *hTERT* was determined by qRT-PCR, and positive expression of all markers was detected in both PBIECs and BIECs-21(Figure 4A and C). The positive expression of *hTERT* mRNA was detected in BIECs-21(Figure 4B). The results proved that the purified cells and immortalized cell line were bovine intestinal epithelial cells, and that the *hTERT* gene was stable and highly expressed in BIECs-21.

The TEM images showed that the cell structure was intact. There were tight junctions (red arrow) and desmosomes (green arrow) between the cells (Figure 5A). The mitochondria are shown by the yellow arrow in the cytoplasm (Figure 5B).

Growth curves of PBIECs and BIECs-21

Cell proliferation was measured by CCK-8 assay, and the growth curves are shown in Figure 6. The growth curve has an 'S' shape, which conforms to the growth characteristics of epithelial cells. The proliferation ability of BIECs-21 was significantly increased compared with PBIECs (Figure 6). These results suggested that BIECs-21 are immortal, since they can continuously proliferate and have good viability.

Karyotype analysis of BIECs-21

Karyotyping of BIECs-21 indicated that the cells contained 60 chromosomes, consistent with a diploid karyotype (Figure 7A and B). Except for X and Y staining, there was no significant difference in the position and number of G-banding of

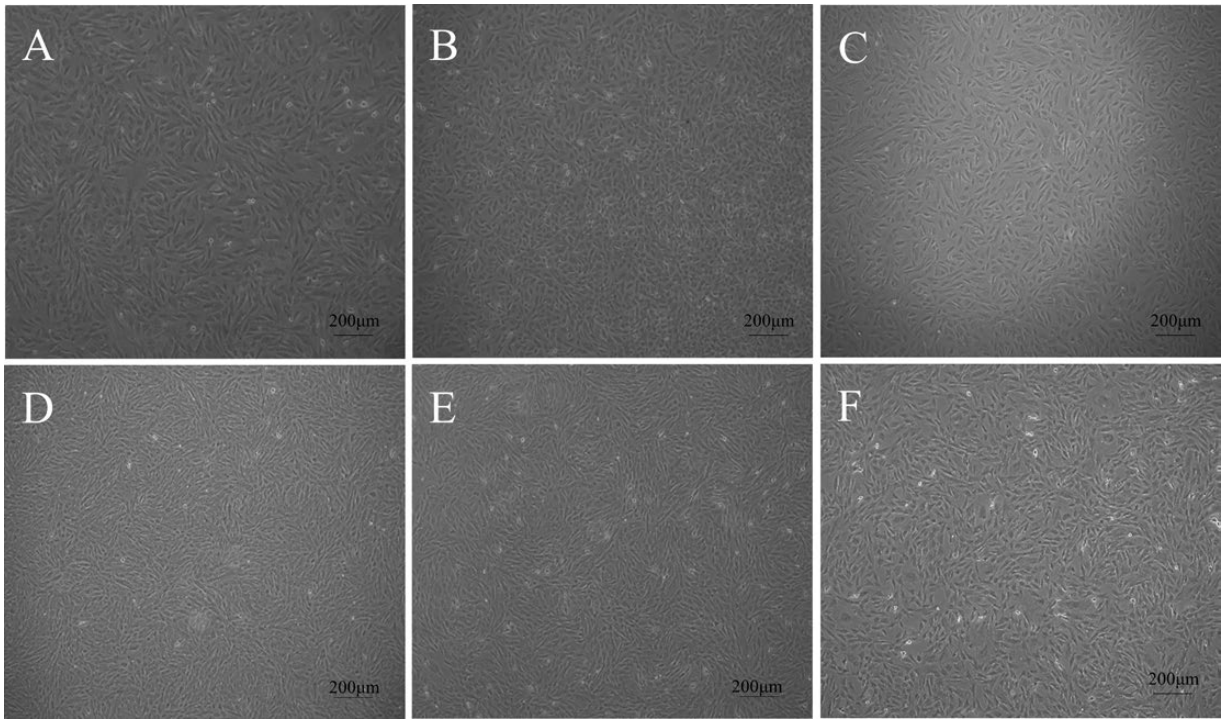

Figure 2. Morphology of immortalized cells after continuous passage. (A, B, C, D, E, and F) After hTERT transfection into primary BIECs and selection by incubation in the presence of G418. The morphology of the immortalized cells was imaged at passages 5, 9, 14, 21, 28, and 36 (50×). hTERT: human telomerase reverse transcriptase; G418: geneticin.

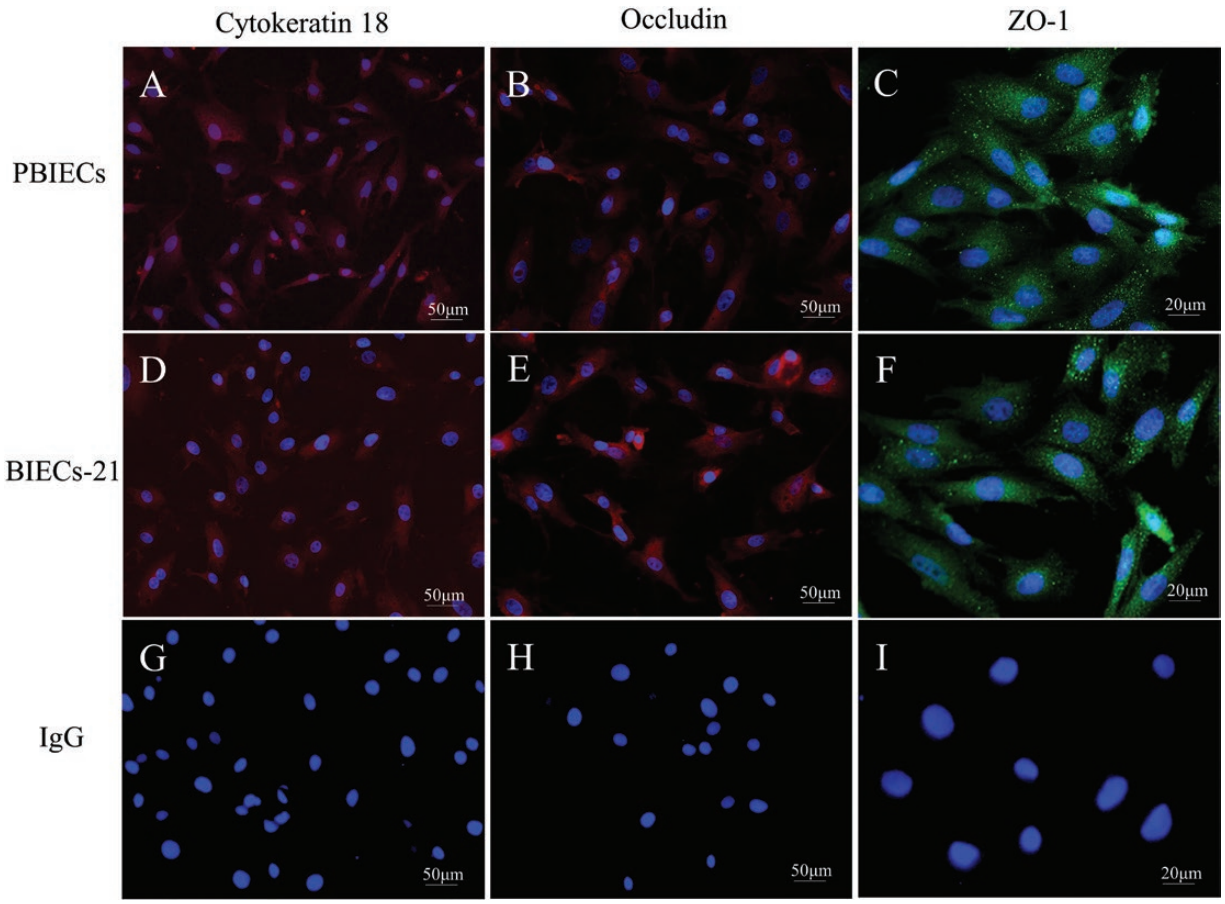

Figure 3. Immunofluorescence identification of PBIECs and BIECs-21. (A and D) Immunostaining of PBIECs and BIECs-21 for cytokeratin 18 (200×); (B and E) immunostaining of PBIECs and BIECs-21 for occludin (200×); (C and F) immunostaining of PBIECs and BIECs-21 for zonula occludens-1 (ZO-1) (400×); (G, H, and I) negative controls without first antibody for cytokeratin 18, occludin and ZO-1. PBIECs: primary bovine intestinal epithelial cells; BIECs-21: immortalized bovine intestinal epithelial cell line.

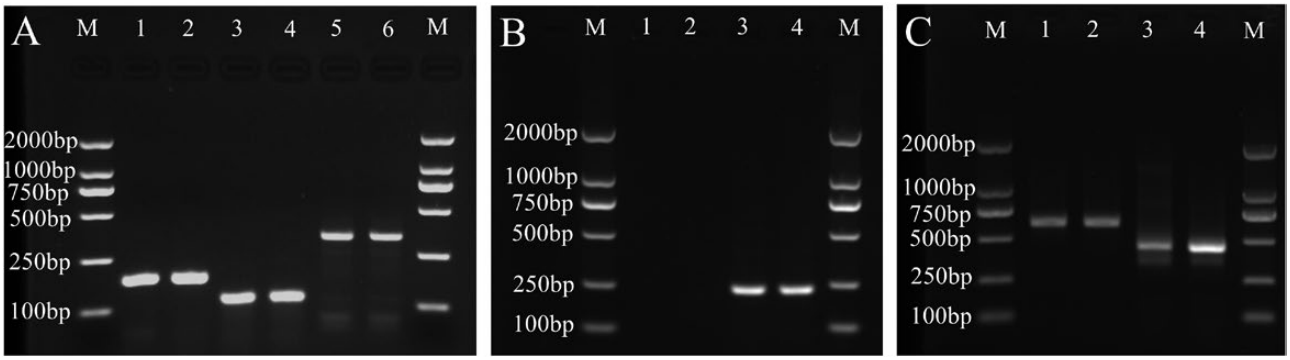

Figure 4. Reverse-transcriptase polymerase chain reaction (RT-PCR) analysis of specific target gene expression. (A) *CK*18, E-cadherin and enterokinase mRNA expression. Lane M: DNA marker DL2000; lane 1, 3, 5: *CK*18, E-cadherin and enterokinase expressed in PBIECs; lane 2, 4, 6: *CK*18, E-cadherin and enterokinase expressed in BIECs-21; (B) *hTERT* mRNA expression. Lane M: DNA marker DL2000; lane 1: negative control; lane 2: *hTERT* expressed in PBIECs; lane 3: *hTERT* expressed in BIECs-21; lane 4: positive control; (C) Vimentin *and* villin mRNA expression. Lane M: DNA marker DL2000; lane 1, 3: Vimentin *and* villin expressed in PBIECs; lane 2, 4: Vimentin *and* villin expressed in BIECs-21. PBIECs: primary bovine intestinal epithelial cells; BIECs-21: immortalized bovine intestinal epithelial cell line.

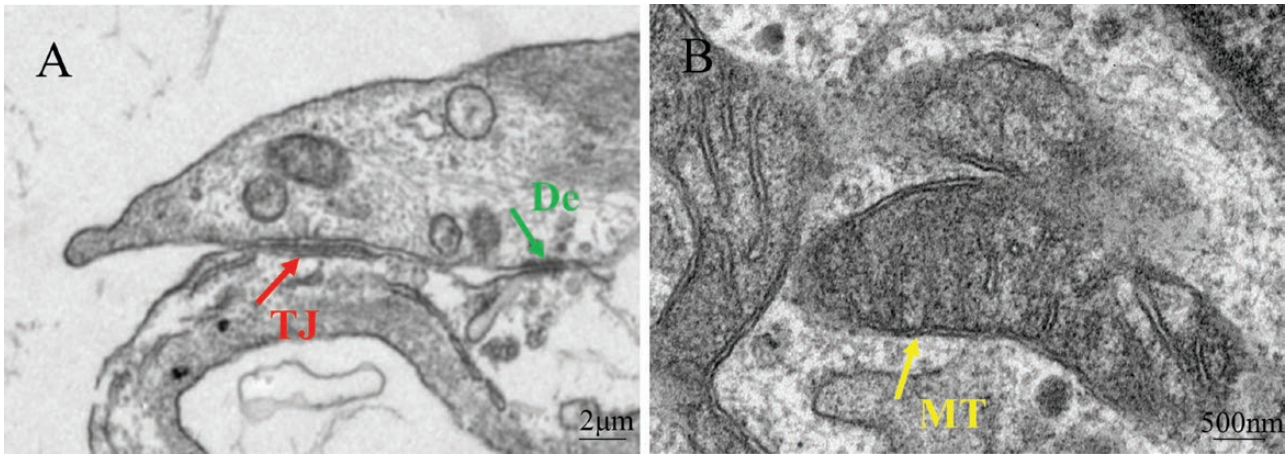

Figure 5. Transmission electron microscope images of BIECs-21. (A) 7,000×; (B) 20,000×. TJ: tight junction (arrow on the left in Figure A); De: desmosome (arrow on the right in Figure A); MT: mitochondrion (arrow in Figure B).

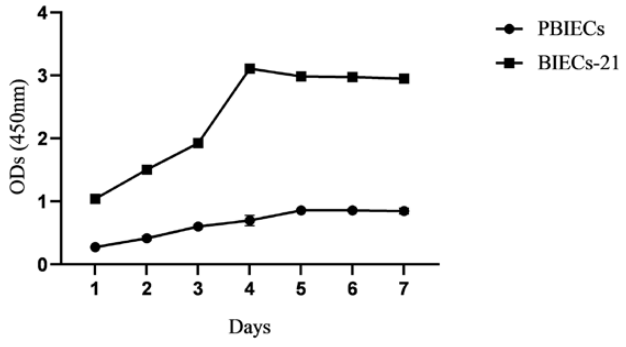

Figure 6. Growth curves of PBIECs and BIECs-21. PBIECs: primary bovine intestinal epithelial cells; BIECs-21: immortalized bovine intestinal epithelial cell line.

autosomes (Figure 7C and D). The results showed that the BIECs-21 were genetically stable.

Uptake of SCFAs

Cell viability was measured after treating the BIECs-21 with SCFAs at increasing concentrations (30, 60, 90, 120, 150, and 180 mM) for 24 h. The SCFAs significantly promoted cell viability at 30 ($P < 0.001$), 60 ($P < 0.001$), and 90 mM ($P < 0.05$) compared with the control; However, SCFAs significantly suppressed cell viability at 120, 150, and 180 mM compared with control ($P < 0.001$; Figure 8A). The 30 mM SCFA concentration was selected for incubation with the PBIECs and BIECs-21 to verify the transporter function. The SCFAs significantly increased mRNA expression of *MCT*-1 ($P < 0.01$), *MCT*-4 ($P < 0.001$), *GPR*41 ($P < 0.05$) and *SLC5A*8 ($P < 0.001$) compared with the control group in primary cells (Figure 8B). The SCFAs significantly increased mRNA expression of *MCT*-1, *MCT*-4, *GPR*41, *GPR*43 and *SLC5A*8 in BIECs-21 compared with the control group ($P < 0.001$; Figure 8C), which showed the same trend as PBIECs. The results showed that the immortalized cells had normal SCFA transporter function.

Uptake of glucose

The glucose concentration in the culture supernatants was measured after incubating PBIECs and BIECs-21 with low (5.55 mM) glucose for 24 h compared to medium alone. The glucose content in the supernatants was significantly lower than in the culture medium ($P < 0.001$; Figure 9A and B) and

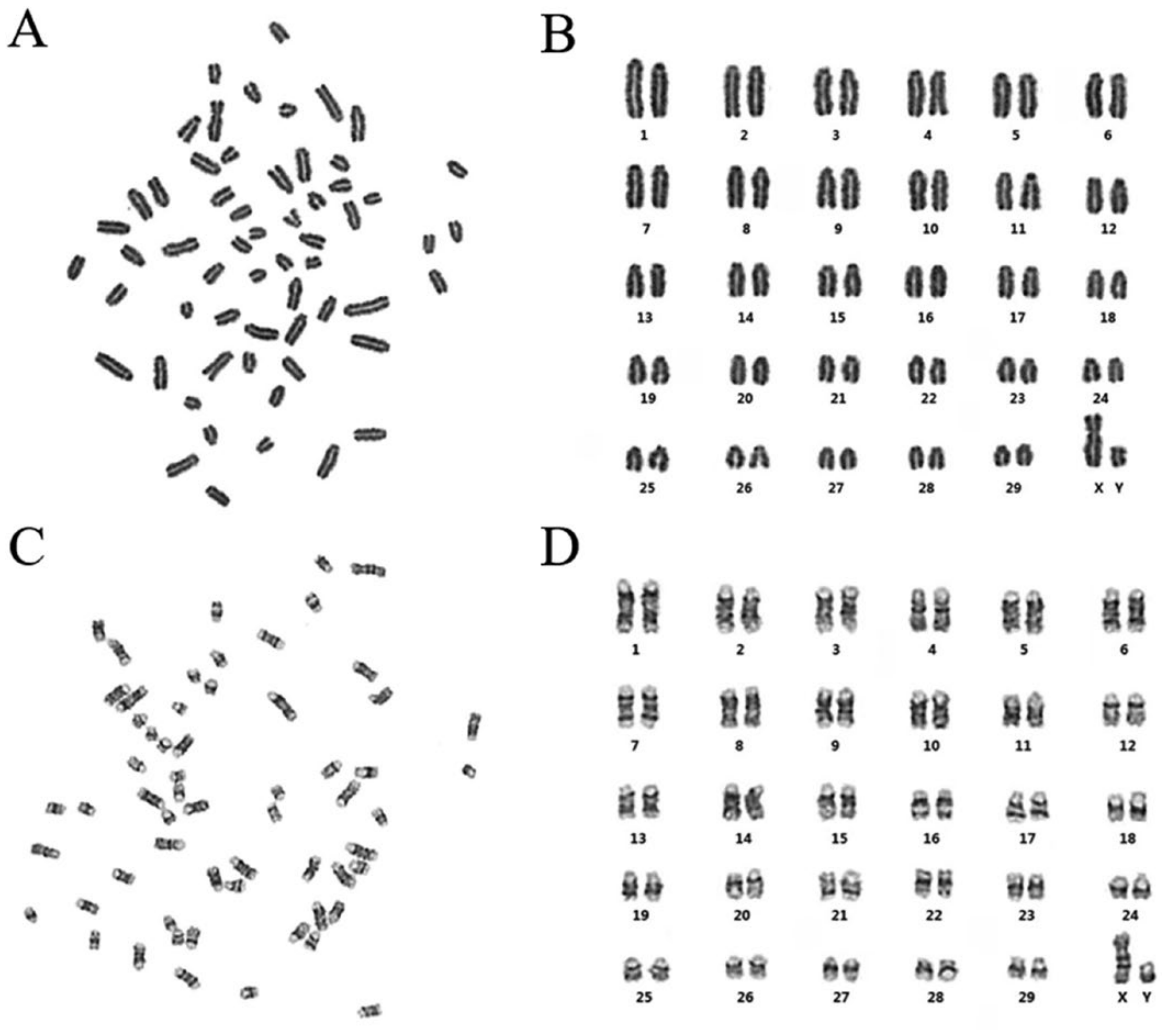

Figure 7. Karyotype analysis of BIECs-21. (A) Karyotyping of BIECs-21; (B) chromosomal rearrangements of BIECs-21; (C) G-banding analysis of BIECs-21; (D) chromosomal rearrangements with G-banding of BIECs-21. BIECs-21: immortalized bovine intestinal epithelial cell line.

the 5.55 mM glucose concentration was selected to test the glucose absorption of the PBIECs and BIECs-21. The glucose significantly increased the mRNA expression of SGLT1 ($P < 0.01$), GLUT2 ($P < 0.001$), and *GLUT5* ($P < 0.01$) compared with the control group for primary cells (Figure 9C). Glucose significantly increased mRNA expression of *SGLT*1 ($P < 0.001$), *GLUT*2 ($P < 0.001$), and *GLUT5* ($P < 0.01$) compared with the control group for BIECs-21 (Figure 9D), which showed the same trend with the PBIECs. The results showed that the BIECs-21 had normal glucose absorption.

Analysis of serum dependence

The PBIECs and BIECs-21 cannot grow normally in culture medium without FBS, which promoted growth in a concentration-dependent manner (Figure 10). The dependence of BIECs-21 on serum did not change during passage, indicating that the cells did not undergo carcinogenesis.

Analysis of contact inhibition

The BIECs-21 entered the plateau stage after 2 to 3 d of logarithmic growth. At that time, the cells were approaching confluence and the proliferation rate was decreasing (Figure 11A). The cells reached the confluent state on the fifth day without undergoing multiple layer growth (Figure 11B). The cells began to detach on the eighth day, and the phenomenon of a pulling network appeared (Figure 11C). This result indicates that BIECs-21 still had contact inhibition.

Growth state of Nc-1 and GFP-Nc infecting BIECs-21

The BIECs-21 were infected with *Neospora caninum* (Nc-1 and GFP-Nc) at a ratio of 3:1 (parasites:cells). Compared with the control group, the morphology of the infected BIECs-21 deteriorated (Figure 12A and E). The Nc-1 and GFP-Nc began to enter the cells 3 h after infection. After 12 h, most of the Nc-1 (Figure 12B) and GFP-Nc (Figure 12F) had entered the cells, and about half of the vacuoles contained two tachyzoites. After 24 h, Nc-1 and GFP-Nc showed different degrees of partitioning with most of the vacuoles containing four tachyzoites. About 36 h after infection of BIECs-21 with Nc-1 or GFP-Nc, large parasitophorous vacuoles containing numerous tachyzoites were formed in cells (Figure 12C and G). After about 48 h, some parasitophorous vacuoles burst, the tachyzoites were released, and the damaged cells detached (Figure 12D and H).

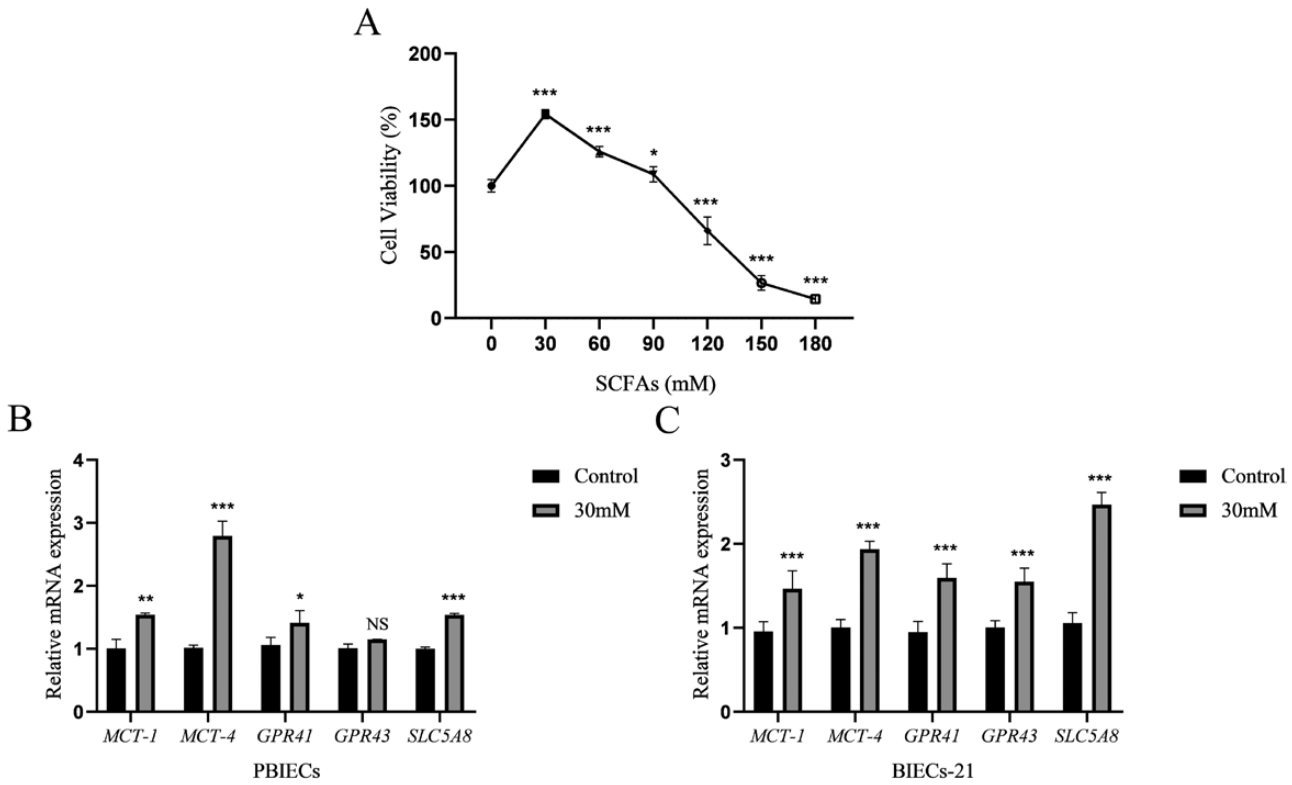

Figure 8. Effect of SCFAs on viability and assay of SCFA uptake. (A) Cell viability was measured after incubating BIECs-21 with SCFAs at increasing concentrations (30, 60, 90, 120, 150, and 180 mM) for 24 h. SCFAs include sodium acetate, sodium propionate, and sodium butyrate (at a ratio of 14:5:1). Data are given as a percentage of the control group values. (B) Effect of 30 mM SCFAs on the mRNA expression of monocarboxylate transporter-1 (*MCT-1*), monocarboxylate transporter-4 (*MCT-4*), G protein-coupled receptor 41 (*GPR41*), G protein-coupled receptor 43 (*GPR43*) and sodium-dependent monocarboxylate transporter (*SCL5A8*) after incubation with PBIECs for 24 h. (C) Effect of 30 mM SCFA on mRNA expression of *MCT-1*, *MCT-4*, *GPR41*, *GPR43* and *SCL5A8* after incubation with BIECs-21 for 24 h. The control group was normal cells with no SCFAs. Values are mean ± SD ($n = 6$). Statistical significance was calculated by Student's *t* test (Figure 8B and C) and one-way ANOVA with a Duncan test (Figure 8A). Significance: $^{*}P < 0.05$, $^{**}P < 0.01$, $^{***}P < 0.001$. NS, no significant differences. PBIECs: primary bovine intestinal epithelial cells; BIECs-21: immortalized bovine intestinal epithelial cell line.

Discussion

The intestine is the primary organ of nutrient absorption and metabolism in ruminants (Sanz-Fernandez et al., 2020), and the mucosal surfaces of the intestinal tract are constantly exposed to commensal and potentially pathogenic microorganisms, leading to the occurrence of many intestinal diseases (Peng et al., 2019). Thus, it is essential for the study of the pathogenesis of intestinal diseases and drug intervention to establish a stable immortalized BIECs cell line with suitable culture methods.

The most common methods for primary culture of IECs are enzymatic digestion with collagenase, trypsin, or neutral protease or a combination of these, chelation, and tissue mass culture (Tang et al., 2017). Collagenase digestion is recognized as the most efficient method (Zhan et al., 2020), but, fibroblasts are often mixed in with the primary IECs. At present, manual scraping, differential digestion, differential adhesion and monoclonal culture method are commonly used to purify primary epithelial cells (Wang et al., 2014; Cui et al., 2019; Zhang et al., 2019; Wu et al., 2022). In this study, the PBIECs were isolated with type I collagenase from the intestinal epithelial tissues of a calf, and the epithelial cells were treated by the differential digestion and differential adhesion method to obtain high-purity PBIECs.

After a limited number of passages, the primary IECs will stop dividing and enter a senescent state (Wang et al., 2022b), after which they do not proliferate further (Zhan et al., 2017). In addition, the isolation and culture of primary cells is laborious and time-consuming, and the metabolic status of each batch can differ (Burek et al., 2012). Therefore, the establishment of an immortalized IEC line is particularly important for scientific studies. The fundamental cause of replicative senescence of cells is thought to be the gradual shortening of telomeres (Jack et al., 2022). Activation of telomerase, a ribonucleoprotein, involved in telomere synthesis (Kim and Kislinger, 2013), can enable cells to escape senescence and acquire the ability to proliferate indefinitely (Chen et al., 2019). Stable introduction of exogenous *hTERT*, the catalytic component of telomerase, increases telomerase activity (Bodnar et al., 1998). Recently, an immortalized bovine intestinal epithelial cell line established by transfecting ileum IECs with the *hTERT* gene was reported (Katwal et al., 2019). Furthermore, a bovine intestinal epithelial cell line has been established by transfecting duodenal epithelial cells with the SV40 large T antigen gene (Miyazawa et al., 2010). However, in this report, the *hTERT* gene was successfully transferred into primary duodenal epithelial cells along with G418 resistance to obtain an immortalized cell line stably expressing the *hTERT* gene. This cell line can be used for in vitro studies of the common functions of different intestinal tracts, but not the specific functions of the jejunum, ileum, or colon.

After G418 screening treatment, it was found that the newly established BIECs-21 retained the morphological and

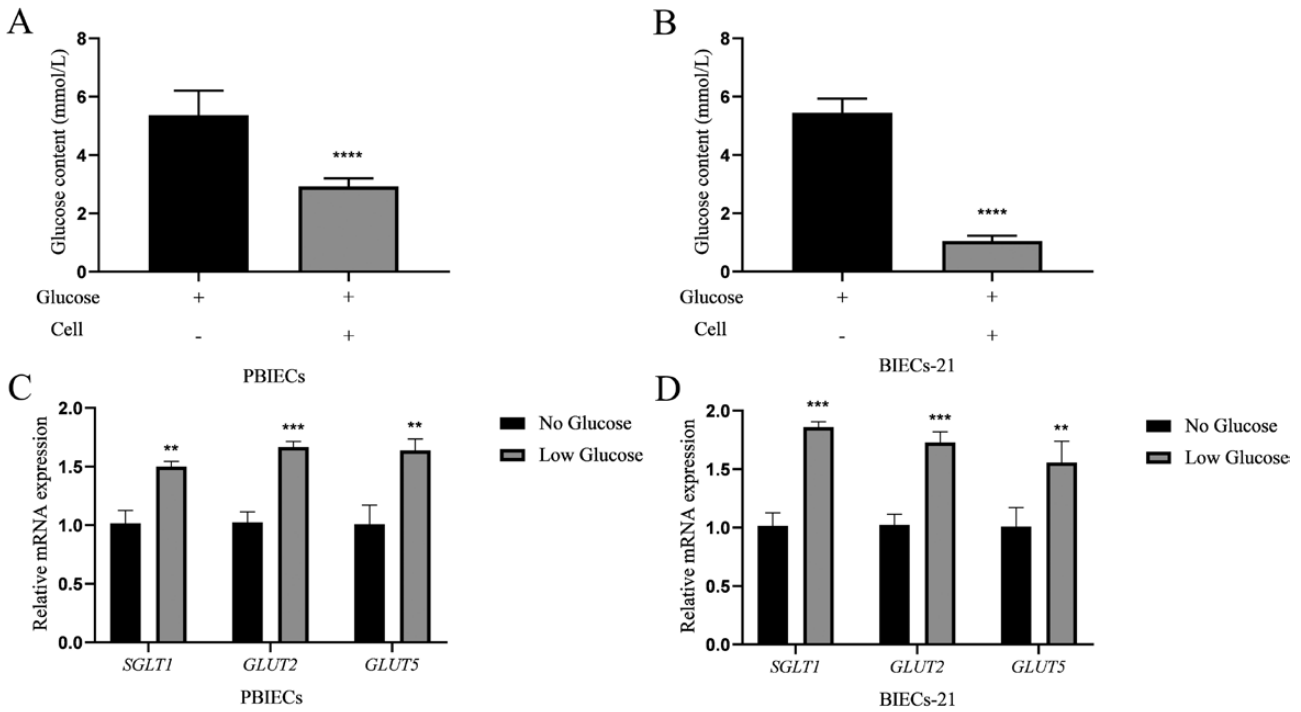

Figure 9. Analysis of glucose uptake. (A) Glucose content in culture supernatants of PBIECs incubated in low glucose (5.55 mM) medium for 24 h. (B) Glucose content in culture supernatants of BIECs-21 incubated in low glucose medium for 24 h. (C) Effect of low-glucose medium on mRNA expression of sodium glucose cotransporters 1 (*SGLT1*), glucose transporter 2 (*GLUT2*) and glucose transporter 5 (*GLUT5*) after incubation of PBIECs for 24 h. (D) Effect of low-glucose medium on mRNA expression of sodium glucose cotransporters 1 (*SGLT1*), glucose transporter 2 (*GLUT2*) and glucose transporter 5 (*GLUT5*) after incubation of the BIECs-21 for 24 h. The control group was normal cells with no glucose. Values are mean ± SD (n = 6). Statistical significance was calculated by Student's t test. Significance: *P < 0.05, **P < 0.01, ***P < 0.001. PBIECs: primary bovine intestinal epithelial cells; BIECs-21: immortalized bovine intestinal epithelial cell line.

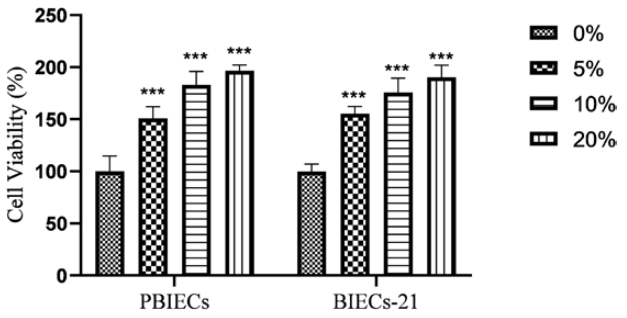

Figure 10. Serum dependence of PBIECs and BIECs-21. Cell viability was measured after incubating PBIECs and BIECs-21 in medium containing increasing concentrations of FBS (0%, 5%, 10%, and 20%) for 48 h. The data are expressed as a percentage of the control group values (mean ± SD, n = 6). Statistical significance was calculated by one-way ANOVA with a Duncan test. Significance: *P < 0.05, **P < 0.01, ***P < 0.001. PBIECs: primary bovine intestinal epithelial cells; BIECs-21: immortalized bovine intestinal epithelial cell line.

functional characteristics of PBIECs. RT-PCR results showed that *hTERT* mRNA was positively expressed in BIECs-21 and negatively expressed in PBIECs. CK18 is a member of the family of type I keratins and an important protein marker for identifying epithelial cells (Yamada et al., 2021). In this study, the expression of CK18 was detected in both PBIECs and BIECs-21, confirming the epithelial origin of the cells. The tight junction proteins, ZO-1 and occludin, and the junction protein, E-cadherin, are critical epithelial cell molecular markers and essential components of the intestinal barrier (Zou et al., 2020; Xi et al., 2022). In this study, occludin, ZO-1, and E-cadherin were positively expressed in both PBIECs and BIECs-21, indicating that BIECs-21 retained intestinal epithelial cell characteristics similar to PBIECs. Enterokinase is a proteolytic enzyme, mainly localized to the brush-border membrane of IECs (Prohaska et al., 2012). Villin is a structural component of microvilli forming the brush border of the small intestine and plays a key role in maintaining brush border organization (Athman et al., 2002). We found that enterokinase and villin were expressed in both PBIECs and BIECs-21, indicating that BIECs-21 still expressed intestinal epithelial cell-specific proteins, and could produce peptides by using intestinal peptidase to hydrolyze proteins. Vimentin, a type III intermediate filament protein, is expressed in mesenchymal cells (Kumar et al., 2022). Re-expression of vimentin in epithelial cells has been reported (Evans et al., 1992). Vimentin re-expression in vitro may help maintain cellular structure and/or function of specific proteins (Rusu et al., 2005). Tight junctions and desmosomes are typical features of IECs (Chen et al., 2022). We observed mitochondria in the cytoplasm, and tight junctions and desmosomes between cells of the BIECs-21 by transmission electron microscopy, indicating that BIECs-21 had complete intestinal epithelial cell structure and normal organelles. These results confirmed the intestinal epithelial origin of the newly established cell line.

The growth curve of both PBIECs and BIECs-21 presented an 'S' shape, which conformed to the growth law of epithelial cells. However, the proliferation ability of BIECs-21 was enhanced, and the time of entering the plateau stage was earlier compared with that of primary cells. These results suggest that immortalized cell lines have strong cell viability. The BIECs-21 contained 60 chromosomes, consistent with a

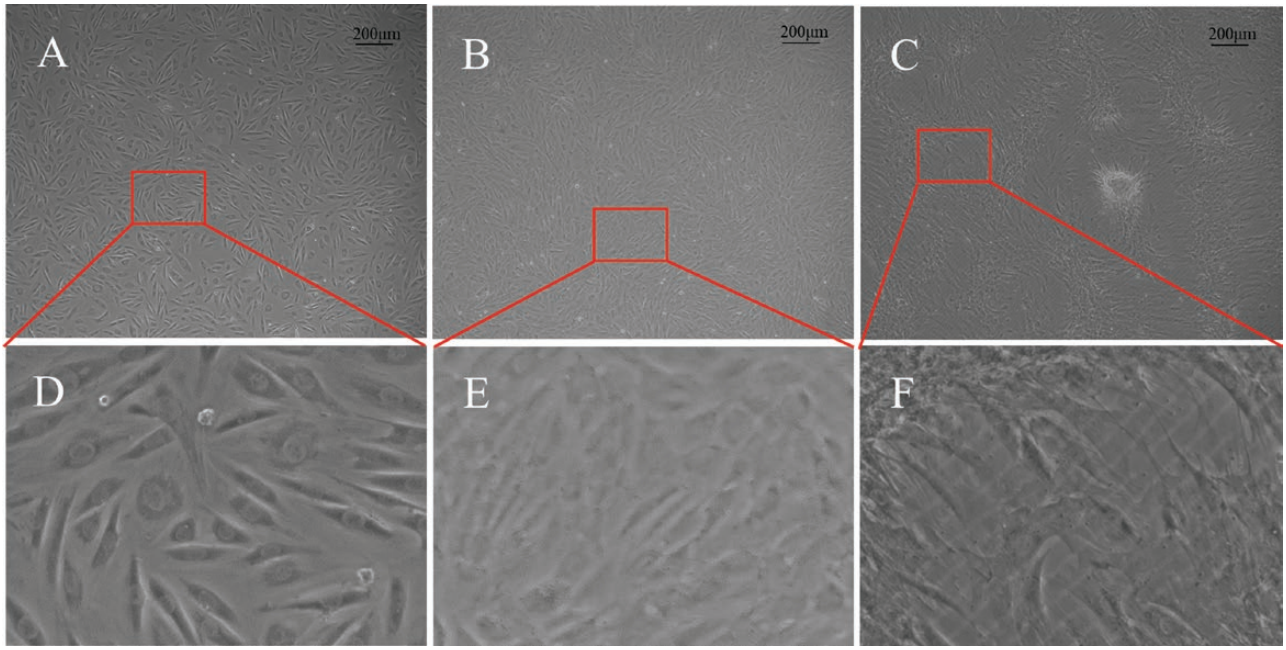

Figure 11. Analysis of contact inhibition. (A and D) BIECs-21 approaching confluence (50×); (B and E) BIECs-21 at confluence (50×). (C and F) BIECs-21 show the phenomenon of the pulling net (50×). BIECs-21: immortalized bovine intestinal epithelial cell line.

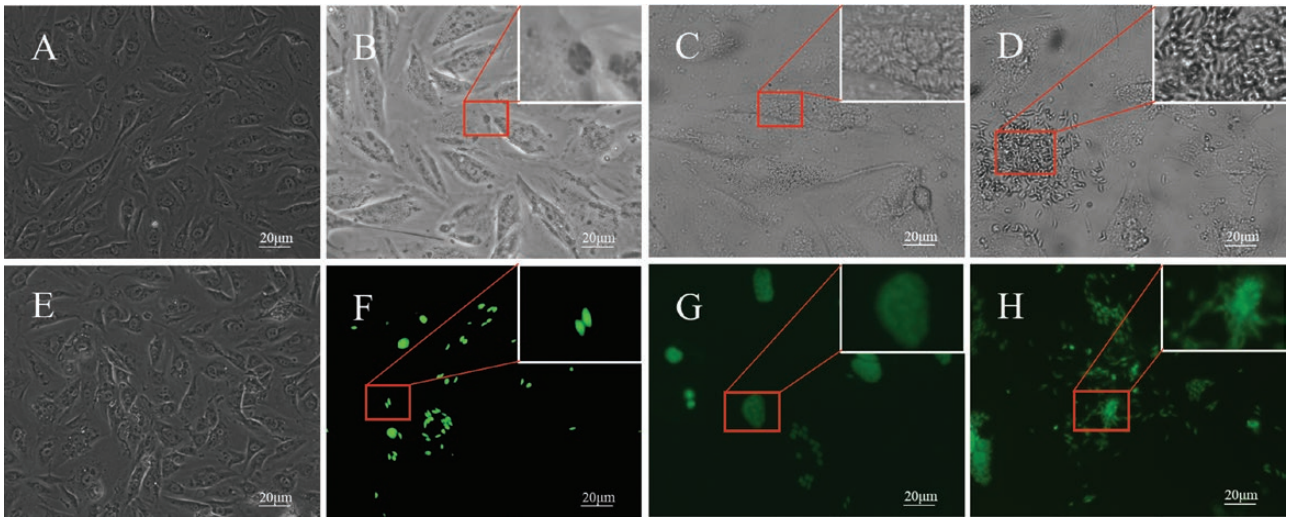

Figure 12. Growth state of Nc-1 and GFP-Nc on BIECs-21. (A and E) Morphology of normal cells without infection compared with cells infected with *Neospora caninum* (Nc; 400×); (B and F) Morphology of cells infected with Nc-1 and GFP-Nc for 12 h (400×); (C and G) Morphology of cells infected with Nc-1 and GFP-Nc for 36 h (400×); (D and H) Morphology of cells infected with Nc-1 and GFP-Nc for 48 h (400×). BIECs-21: immortalized bovine intestinal epithelial cell line.

diploid karyotype, and there was no significant difference in the position and number of G-banding of autosomes except for X and Y staining. The metabolic results showed that the BIECs-21 had stable biological functions. Cancerous cells lose their serum dependence and can grow in multiple layers during unlimited passages in vitro (Ramasamy et al., 2014; Guo et al., 2022b). The BIECs-21 were serum-dependent and did not proliferate well under serum-free or low-serum conditions, similar to PBIECs. And both PBIECs and BIECs-21 had the property of contact inhibition. These results indicated that BIECs-21 had no overt tumor cell characteristics after many passages—the cell line has been passed more than 80 times.

From 15% to 50% of SCFAs can reach the small intestine in ruminants (Zhan et al., 2020). SCFAs are absorbed in the intestine through the intracellular transmembrane transport of *MCT*-1 and *MCT*-4 (Jardou et al., 2021), and into the blood circulation via *SLC5A*8, a solute carrier (**SLC**) family transporter (Gu et al., 2021). Various studies have shown that SCFAs regulate host energy metabolism, immune responses and inflammation via *GPR*41 and *GPR*43, SCFA receptors (Natarajan et al., 2016). In this study, SCFAs increased the expression of *MCT*-1, *MCT*-4, *GPR*41, *GPR*43 and *SLC5A*8 in PBIECs and BIECs-21, indicating that the immortalized cell lines had normal SCFA transport function. The absorption of glucose is one of the main functions of the small intestinal

epithelium (Hussar et al., 2020). *SGLT*1, a primary glucose transporter, is considered to be the major route for absorption of glucose in the IECs (Chen et al., 2018). Glucose is absorbed through *SGLT*1 in the brush-border membrane and passed into the blood circulation via *GLUT*2, a member of the facilitative glucose transporter family (Dai et al., 2016). *GLUT5*, another member of the glucose transporter family, specifically absorbs fructose from the intestine and transports it into the bloodstream (Krause and Wegner, 2020). Our data show that glucose induced the expression of *SGLT*1, *GLUT*2 and *GLUT5* in PBIECs and BIECs-21, indicating that the immortalized cell line possessed the normal biological functions of IECs including sugar absorption. Although this cell line is derived from the duodenum of a newborn calf, it retains important functions of IECs.

We found that the newly established BIECs-21 cell line was not transformed, and that this cell line retained the specific physiological functions of bovine intestinal epithelial cells in vivo, which confirms its usefulness as a model for research on intestinal pathology. Previous studies have shown that Nc sporozoites can invade bovine intestinal epithelial cells causing miscarriage and stillbirth in cows and neurological disease in calves (Jia et al., 2013). There has been no bovine small intestinal epithelial cell line for use in research, which has hindered studies of Nc pathogenesis. Here we report on the creation of BIECs-21, a non-transformed, immortalized BIEC line with normal characteristics of epithelial cells. Our results showed that Nc could infect BIECs-21 and proliferate in the cells, indicating that they could be used as a model of Nc infection for further research on the mechanism of infection.

Conclusions

In summary, we developed the BIECs-21 cell line by transfecting PBIECs with an expression vector carrying the *hTERT* gene. The newly established BIECs-21 cell line was not transformed and can be safely used for future studies as it retains the morphological and functional features of PBIECs. Thus, BIECs-21 provides an essential experimental model for studying bovine intestinal diseases.

Supplementary Data

Supplementary data are available at *Journal of Animal Science* online.

Acknowledgments

This study was supported by the National Natural Science Foundation of China (31872537; 31402263), and the National Key Research and Development Program of China (2017YFE0129900). We thank the teachers and students of the College of Animal Science and Technology, Henan University of Science and Technology, for their help. We also thank Professor Qun Liu of the College of Veterinary Medicine, China Agricultural University, for donating Nc-1 and GFP-Nc.

Conflict of Interest Statement

In this study, the authors asserted that they had no conflict of interest.

Literature Cited

Athman, R., D. Louvard, and S. Robine. 2002. The epithelial cell cytoskeleton and intracellular trafficking. III. How is villin involved in the actin cytoskeleton dynamics in intestinal cells? *Am. J. Physiol. Gastrointest. Liver Physiol.* 283:G496–G502. doi:10.1152/ajpgi.00207.2002.

Blackburn, E. 1991. Structure and function of telomeres. *Nature* 350:569–573. doi:10.1038/350569a0.

Bodnar, A. G., M. Ouellette, M. Frolkis, S. E. Holt, C. P. Chiu, G. B. Morin, C. B. Harley, J. W. Shay, S. Lichtsteiner, and W. E. Wright. 1998. Extension of life-span by introduction of telomerase into normal human cells. *Science* 279:349–352. doi:10.1126/science.279.5349.349.

Burek, M., E. Salvador, and C. Y. Förster. 2012. Generation of an immortalized murine brain microvascular endothelial cell line as an in vitro blood brain barrier model. *J. Vis. Exp* 29:e4022. doi:10.3791/4022.

Chen, X. 2019. *Repairment of glutamic acid on the damage by heat stress in dairy cattle intestinal epithelial cells*. MA thesis, Henan University of Science and Technology.

Chen, C., Y. Yin, Q. Tu, and H. Yang. 2018. Glucose and amino acid in enterocyte: absorption, metabolism and maturation. *Front. Biosci. (Landmark Ed.)* 23:1721–1739. doi:10.2741/4669.

Chen, Y., S. Hu, M. Wang, B. Zhao, N. Yang, J. Li, Q. Chen, M. Liu, J. Zhou, G. Bao, et al. 2019. Characterization and establishment of an immortalized rabbit melanocyte cell line using the SV40 large T antigen. *Int. J. Mol. Sci.* 20:4874. doi:10.3390/ijms20194874.

Chen, Y., X. Wang, C. Zhang, Z. Liu, C. Li, and Z. Ren. 2022. Gut microbiota and bone diseases: a growing partnership. *Front. Microbiol.* 13:877776. doi:10.3389/fmicb.2022.877776.

Cruz-Vázquez, C., J. Vital-Gutiérrez, L. Medina-Esparza, L. Ortega-Mora, A. Valdivia-Flores, T. Quezada-Tristán, and A. Orihuela-Trujillo. 2017. *Neospora caninum* infection during the first gestation of Holstein heifers that consume food contaminated naturally with Zearalenone under field conditions. *Iran. J. Parasitol.* 12:563–571.

Cui, H., W. Liang, D. Wang, K. Guo, and Y. Zhang. 2019. Establishment and characterization of an immortalized porcine oral mucosal epithelial cell line as a cytopathogenic model for porcine circovirus 2 infection. *Front. Cell. Infect. Microbiol.* 9:171. doi:10.3389/fcimb.2019.00171.

Dai, L., W. W. Hu, L. Xia, M. Xia, and Q. Yang. 2016. transmissible gastroenteritis virus infection enhances SGLT1 and GLUT2 expression to increase glucose uptake. *PLoS One* 11:e0165585. doi:10.1371/journal.pone.0165585.

Emami, S., L. Mir, C. Gespach, and G. Rosselin. 1989. Transfection of fetal rat intestinal epithelial cells by viral oncogenes: establishment and characterization of the E1A-immortalized SLC-11 cell line. *Proc. Natl. Acad. Sci. U.S.A.* 86:3194–3198. doi:10.1073/pnas.86.9.3194.

Evans, G. S., N. Flint, A. S. Somers, B. Eyden, and C. S. Potten. 1992. The development of a method for the preparation of rat intestinal epithelial cell primary cultures. *J. Cell Sci.* 101:219–231. doi:10.1242/jcs.101.1.219.

Franke, W. W., B. Appelhans, E. Schmid, C. Freudenstein, M. Osborn, and K. Weber. 1979. Identification and characterization of epithelial cells in mammalian tissues by immunofluorescence microscopy using antibodies to prekeratin. *Differentiation*. 15:7–25. doi:10.1111/j.1432-0436.1979.tb01030.x.

Gu, B. H., M. Kim, and C. H. Yun. 2021. Regulation of gastrointestinal immunity by metabolites. *Nutrients*. 13:167. doi:10.3390/nu13010167.

Guo, D., L. Zhang, X. Wang, J. Zheng, and S. Lin. 2022a. Establishment methods and research progress of livestock and poultry immortalized cell lines: a review. *Front. Vet. Sci.* 9:956357. doi:10.3389/fvets.2022.956357.

Guo, L., Z. Wang, J. Li, J. Li, L. Cui, J. Dong, X. Meng, C. Qian, and H. Wang. 2022b. Immortalization effect of SV40T lentiviral vectors on canine corneal epithelial cells. *BMC Vet. Res.* 18:181. doi:10.1186/s12917-022-03288-3.

Hayflick, L. 1997. Mortality and immortality at the cellular level. A review. *Biochemistry.* 62:1180–1190.

Ho, C., H. Chiang, S. Li, C. Yuan, and H. Ng. 1987. Establishment and characterization of a tumorigenic trophoblast-like cell line from a human placenta. *Cancer Res.* 47:3220–3224.

Hussar, P., F. Popovska-Percinic, K. Blagoevska, T. Järveots, and I. Dūrītis. 2020. Immunohistochemical study of glucose transporter GLUT-5 in duodenal epithelium in norm and in T-2 mycotoxicosis. *Foods.* 9:849. doi:10.3390/foods9070849.

Jack, A., Y. Kim, A. R. Strom, D. S. W. Lee, B. Williams, J. M. Schaub, E. H. Kellogg, I. J. Finkelstein, L. S. Ferro, A. Yildiz, et al. 2022. Compartmentalization of telomeres through DNA-scaffolded phase separation. *Dev. Cell* 57:277–290.e9.e279. doi:10.1016/j.devcel.2021.12.017.

Jardou, M., Q. Provost, C. Brossier, E. Pinault, F. L. Sauvage, and R. Lawson. 2021. Alteration of the gut microbiome in mycophenolate-induced enteropathy: impacts on the profile of short-chain fatty acids in a mouse model. *BMC. Pharmacol. Toxicol.* 22:66. doi:10.1186/s40360-021-00536-4.

Jia, L. J., S. F. Zhang, N. C. Qian, X. N. Xuan, L. Z. Yu, X. M. Zhang, and M. M. Liu. 2013. Generation and immunity testing of a recombinant adenovirus expressing NcSRS2-NcGRA7 fusion protein of bovine *Neospora caninum*. *Korean J. Parasitol.* 51:247–253. doi:10.3347/kjp.2013.51.2.247.

Katwal, P., M. Thomas, T. Uprety, M. B. Hildreth, and R. S. Kaushik. 2019. Development and biochemical and immunological characterization of early passage and immortalized bovine intestinal epithelial cell lines from the ileum of a young calf. *Cytotechnology* 71:127–148. doi:10.1007/s10616-018-0272-y.

Kaul, Z., C. Cheung, P. Bhargava, A. Sari, Y. Yu, H. Huifu, H. Bid, J. Henson, J. Groden, R. Reddel, et al. 2021. Functional characterization of miR-708 microRNA in telomerase positive and negative human cancer cells. *Sci. Rep.* 11:17052. doi:10.1038/s41598-021-96096-y.

Kim, Y., and T. Kislinger. 2013. Novel approaches for the identification of biomarkers of aggressive prostate cancer. *Genome Med.* 5:56. doi:10.1186/gm460.

Kogut, M., A. Lee, and E. Santin. 2020. Microbiome and pathogen interaction with the immune system. *Poult. Sci.* 99:1906–1913. doi:10.1016/j.psj.2019.12.011.

Krause, N., and A. Wegner. 2020. Fructose metabolism in cancer. *Cells.* 9:2635. doi:10.3390/cells9122635.

Kumar, S., R. Verma, N. Tyagi, G. Gangenahalli, and Y. K. Verma. 2022. Therapeutics effect of mesenchymal stromal cells in reactive oxygen species-induced damages. *Hum. Cell* 35:37–50. doi:10.1007/s13577-021-00646-5.

Li, G., J. Shen, J. Cao, G. Zhou, T. Lei, Y. Sun, H. Gao, Y. Ding, W. Xu, Z. Zhan, et al. 2018. Alternative splicing of human telomerase reverse transcriptase in gliomas and its modulation mediated by CX-5461. *J. Exp. Clin. Cancer Res.* 37:78. doi:10.1186/s13046-018-0749-8.

Miyazawa, K., T. Hondo, T. Kanaya, S. Tanaka, I. Takakura, W. Itani, M. T. Rose, H. Kitazawa, T. Yamaguchi, and H. Aso. 2010. Characterization of newly established bovine intestinal epithelial cell line. *Histochem. Cell Biol.* 133:125–134. doi:10.1007/s00418-009-0648-3.

Monteiro, H., Z. Zhou, M. Gomes, P. Peixoto, E. Bonsaglia, I. Canisso, B. Weimer, and F. Lima. 2022. Rumen and lower gut microbiomes relationship with feed efficiency and production traits throughout the lactation of Holstein dairy cows. *Sci. Rep.* 12:4904. doi:10.1038/s41598-022-08761-5.

Natarajan, N., D. Hori, S. Flavahan, J. Steppan, N. A. Flavahan, D. E. Berkowitz, and J. L. Pluznick. 2016. Microbial short chain fatty acid metabolites lower blood pressure via endothelial G protein-coupled receptor 41. *Physiol. Genomics.* 48:826–834. doi:10.1152/physiolgenomics.00089.2016.

O'Sullivan, F., J. Keenan, S. Aherne, F. O'Neill, C. Clarke, M. Henry, P. Meleady, L. Breen, N. Barron, M. Clynes, et al. 2017. Parallel mRNA, proteomics and miRNA expression analysis in cell line models of the intestine. *World J. Gastroenterol.* 23:7369–7386. doi:10.3748/wjg.v23.i41.7369.

Oswald, I. 2006. Role of intestinal epithelial cells in the innate immune defence of the pig intestine. *Vet. Res.* 37:359–368. doi:10.1051/vetres:2006006.

Peng, J., X. Lu, K. Xie, Y. Xu, R. He, L. Guo, Y. Han, S. Wu, X. Dong, Y. Lu, et al. 2019. Dynamic alterations in the gut microbiota of collagen-induced arthritis rats following the prolonged administration of total glucosides of paeony. *Front. Cell. Infect. Microbiol.* 9:204. doi:10.3389/fcimb.2019.00204.

Piñeiro-Ramil, M., C. Sanjurjo-Rodríguez, R. Castro-Viñuelas, S. Rodríguez-Fernández, I. Fuentes-Boquete, F. Blanco, and S. Díaz-Prado. 2019. Usefulness of mesenchymal cell lines for bone and cartilage regeneration research. *Int. J. Mol. Sci.* 20:6286. doi:10.3390/ijms20246286.

Prohaska, T. A., F. C. Wahlmüller, M. Furtmüller, and M. Geiger. 2012. Interaction of protein C inhibitor with the type II transmembrane serine protease enteropeptidase. *PLoS One* 7:e39262. doi:10.1371/journal.pone.0039262.

Quaroni, A., and J. Beaulieu. 1997. Cell dynamics and differentiation of conditionally immortalized human intestinal epithelial cells. *Gastroenterology.* 113:1198–1213. doi:10.1053/gast.1997.v113.pm9322515.

Ramasamy, S., D. Bennet, and S. Kim. 2014. Drug and bioactive molecule screening based on a bioelectrical impedance cell culture platform. *Int. J. Nanomedicine.* 9:5789–5809. doi:10.2147/IJN.S71128.

Rusu, D., S. Loret, O. Peulen, J. Mainil, and G. Dandrifosse. 2005. Immunochemical, biomolecular and biochemical characterization of bovine epithelial intestinal primocultures. *BMC Cell Biol.* 6:42. doi:10.1186/1471-2121-6-42.

Sanz-Fernandez, M., J. Daniel, D. Seymour, S. Kvidera, Z. Bester, J. Doelman, and J. Martín-Tereso. 2020. Targeting the hindgut to improve health and performance in cattle. *Animals (Basel).* 10:1817. doi:10.3390/ani10101817.

Sauriol, A., K. Simeone, L. Portelance, L. Meunier, K. Leclerc-Desaulniers, M. de Ladurantaye, M. Chergui, J. Kendall-Dupont, K. Rahimi, E. Carmona, et al. 2020. Modeling the diversity of epithelial ovarian cancer through ten novel well characterized cell lines covering multiple subtypes of the disease. *Cancers (Basel).* 12:2222. doi:10.3390/cancers12082222.

Shay, J. W., and S. Bacchetti. 1997. A survey of telomerase activity in human cancer. *Eur. J. Cancer (Oxford, England: 1990).* 33:787–791. doi:10.1016/S0959-8049(97)00062-2.

Tang, X., H. Liu, S. Yang, Z. Li, J. Zhong, and R. Fang. 2016. Epidermal growth factor and intestinal barrier function. *Mediators Inflamm.* 2016:1927348. doi:10.1155/2016/1927348.

Tang, Y., W. Xu, W. Guo, M. Xie, H. Fang, C. Chen, and J. Zhou. 2017. [Primary culture of human normal epithelial cells]. *Zhong Nan Da Xue Xue Bao Yi Xue Ban* 42:1327–1333. doi:10.11817/j.issn.1672-7347.2017.11.014.

Tao, D. L., S. S. Zhao, J. M. Chen, X. Chen, X. Yang, J. K. Song, Q. Liu, and G. H. Zhao. 2022. *Neospora caninum* infection induced mitochondrial dysfunction in caprine endometrial epithelial cells via downregulating SIRT1. *Parasit. Vectors.* 15:274. doi:10.1186/s13071-022-05406-4.

Tian, H., H. Wu, G. Wu, and G. Xu. 2020. Noninvasive prediction of TERT promoter mutations in high-grade glioma by radiomics analysis based on multiparameter MRI. *Biomed Res. Int.* 2020:3872314. doi:10.1155/2020/3872314.

Wang, J., G. Hu, Z. Lin, L. He, L. Xu, and Y. Zhang. 2014. Characteristic and functional analysis of a newly established porcine small intestinal epithelial cell line. *PLoS One* 9:e110916. doi:10.1371/journal.pone.0110916.

Wang, R., G. Chu, X. Wang, J. Wu, P. Hu, A. Multani, S. Pathak, H. Zhau, and L. Chung. 2019. Establishment and characterization of a prostate cancer cell line from a prostatectomy specimen for the study of cellular interaction. *Int. J. Cancer* 145:2249–2259. doi:10.1002/ijc.32370.

Wang, J., R. Hu, Z. Wang, Y. Guo, S. Wang, H. Zou, Q. Peng, and Y. Jiang. 2022a. Establishment of immortalized yak ruminal epithelial cell lines by lentivirus-mediated SV40T and hTERT gene transduction. *Oxid. Med. Cell. Longev*. 2022:8128028. doi:10.1155/2022/8128028.

Wang, J., X. Yu, S. Zhao, N. Zhang, Z. Lin, Z. Wang, J. Ma, Y. Yan, J. Sun, and Y. Cheng. 2022b. Construction of a peacock immortalized fibroblast cell line for avian virus production. *Poult. Sci.* 101:102147. doi:10.1016/j.psj.2022.102147.

Whitehead, R., P. VanEeden, M. Noble, P. Ataliotis, and P. Jat. 1993. Establishment of conditionally immortalized epithelial cell lines from both colon and small intestine of adult H-2Kb-tsA58 transgenic mice. *Proc. Natl. Acad. Sci. U.S.A.* 90:587–591. doi:10.1073/pnas.90.2.587.

Wu, X., J. Zhang, S. Yang, Z. Kuang, G. Tan, G. Yang, Q. Wei, and Z. Guo. 2017. Telomerase antagonist imetelstat increases radiation sensitivity in esophageal squamous cell carcinoma. *Oncotarget*. 8:13600–13619. doi:10.18632/oncotarget.14618.

Wu, Y., Z. Wang, G. Hu, and T. Zhang. 2022. Isolation and culture of rat intestinal mucosal microvascular endothelial cells using immunomagnetic beads. *J. Immunol. Methods*. 507:113296. doi:10.1016/j.jim.2022.113296.

Xi, M., P. Zhao, F. Li, H. Bao, S. Ding, L. Ji, and J. Yan. 2022. MicroRNA-16 inhibits the TLR4/NF-κB pathway and maintains tight junction integrity in irritable bowel syndrome with diarrhea. *J. Biol. Chem*. 298:102461. doi:10.1016/j.jbc.2022.102461.

Yamada, M., A. Eguchi, K. Okuno, K. Sakaguchi, and T. Yamaguchi. 2021. Development of a highly sensitive chemiluminescent enzyme immunoassay for fragmented cytokeratin 18 using new antibodies. *Sci. Rep*. 11:18187. doi:10.1038/s41598-021-97439-5.

Zakrzewski, S., J. Richter, S. Krug, B. Jebautzke, I. Lee, J. Rieger, M. Sachtleben, A. Bondzio, J. Schulzke, M. Fromm, et al. 2013. Improved cell line IPEC-J2, characterized as a model for porcine jejunal epithelium. *PLoS One* 8:e79643. doi:10.1371/journal.pone.0079643.

Zhan, K., M. Lin, M. Liu, Y. Sui, and G. Zhao. 2017. Establishment of primary bovine intestinal epithelial cell culture and clone method. *In Vitro Cell. Dev. Biol. Anim*. 53:54–57. doi:10.1007/s11626-016-0082-5.

Zhan, K., T. Yang, Y. Chen, M. Jiang, and G. Zhao. 2020. Propionate enhances the expression of key genes involved in the gluconeogenic pathway in bovine intestinal epithelial cells. *J. Dairy Sci*. 103:5514–5524. doi:10.3168/jds.2019-17309.

Zhang, C., X. Zhu, Y. Hua, Q. Zhao, K. Wang, L. Zhen, G. Wang, J. Lü, A. Luo, W. C. Cho, et al. 2019. YY1 mediates TGF-β1-induced EMT and pro-fibrogenesis in alveolar epithelial cells. *Respir. Res*. 20:249. doi:10.1186/s12931-019-1223-7.

Zhang, C., S. Meng, Q. Shao, X. Wang, C. Li, W. Chen, Y. Li, S. Huang, and Y. Ma. 2022. Protective effects of monoammonium glycyrrhizinate on fatty deposit degeneration induced in primary calf hepatocytes by sodium oleate administration in vitro. *Res. Vet. Sci*. 150:213–223. doi:10.1016/j.rvsc.2022.05.011.

Zhou, Y. B., H. Zhou, L. Li, Y. Kang, X. Cao, Z. Y. Wu, L. Ding, G. Sethi, and J. S. Bian. 2019. Hydrogen sulfide prevents elastin loss and attenuates calcification induced by high glucose in smooth muscle cells through suppression of Stat3/Cathepsin S signaling pathway. *Int. J. Mol. Sci*. 20:4202. doi:10.3390/ijms20174202.

Zou, X., Y. Wang, Y. Wang, J. Yang, H. Guo, and Z. Cai. 2020. Paeoniflorin alleviates abnormalities in rats with functional dyspepsia by stimulating the release of acetylcholine. *Drug. Des. Devel. Ther*. 14:5623–5632. doi:10.2147/DDDT.S260703.